



131 Hartwell Avenue
Lexington, Massachusetts
02421-3126
USA
Tel: +1 781 761-2288
Fax: +1 781 761-2299
www.aer.com

FINAL REPORT

AQRP Project 20 - 005

Using Satellite Observations to Quantify Surface PM_{2.5} Impacts from Biomass Burning Smoke

Revision 2.0

QA Requirements: Audits of Data Quality: 10% Required

Prepared by:
Archana Dayalu, Matthew Alvarado, and Qiang Sun
Atmospheric and Environmental Research, Inc. (AER)
131 Hartwell Ave.
Lexington, MA 02421
Correspondence to: malvarad@aer.com

Prepared for:
Texas Air Quality Research Program (AQRP)
The University of Texas at Austin
August 31, 2021

Document Change Record

Revision	Revision Date	Remarks
0.1	31 July 2021	Internal Version for Review
1.0	02 August 2021	Draft Version Submitted to AQRP
2.0	31 August 2021	Final Version Submitted to AQRP

Acknowledgements

The preparation of this report is based on work supported by the State of Texas through the Air Quality Research Program administered by The University of Texas at Austin by means of a Grant from the Texas Commission on Environmental Quality.

Disclaimer: The information contained in this report or deliverable has not been evaluated by EPA for this specific application, i.e. the identification of brown carbon aerosols and biomass burning smoke. The research was also funded by a grant from the Texas Air Quality Research Program (AQRP Project 20-005) at The University of Texas at Austin through the Texas Emission Reduction Program (TERP) and the Texas Commission on Environmental Quality (TCEQ). The findings, opinions and conclusions are the work of the author(s) and do not necessarily represent findings, opinions, or conclusions of the AQRP or the TCEQ.

Executive Summary

Biomass burning smoke can have major impacts on surface air quality both near the fires and hundreds of miles downwind. These smoke impacts pose two challenges for air quality managers. First, they want to accurately report the potential smoke impacts in time for the public to take protective actions. Second, they need to estimate the recent impacts of smoke on fine particulate matter (PM_{2.5}) to determine which elevated PM_{2.5} episodes may fall under the US EPA Exceptional Events Rule (EER). The EER determines the conditions under which the US EPA will forgo comparison of policy relevant air monitoring data to a relevant National Ambient Air Quality Standard (NAAQS).

Various satellite observations provide valuable information on the locations of fires and transport of smoke. Existing analysis products, such as the NOAA Hazard Mapping System (HMS) Fire and Smoke product, provide observed fire locations and identify regions that are being impacted by biomass burning smoke. However, there are multiple products that use different techniques to identify smoke plumes, and thus may disagree on the extent of the area covered by biomass burning smoke. In addition, due to the nature of these measurement systems, these products do not currently provide information on the height of the smoke plumes or estimates of the surface impacts of the observed smoke. An analysis of existing smoke products that increases our confidence in the identification of smoke and provides an estimate of smoke height and surface PM_{2.5} impact would greatly help TCEQ air quality managers protect the public and properly enforce air quality standards.

In this project, the AER project team evaluated the ability of three existing remote sensing smoke products to accurately and consistently identify regions impacted by smoke over 93 suspected smoke days in the Texas/Gulf of Mexico region. The team compared and evaluated the smoke products using additional satellite observations that are sensitive to smoke, specifically observations of carbon monoxide (CO), ammonia (NH₃), and proxies for carbon-based aerosols from biomass burning. The team also estimated the heights of smoke plumes detected by the HMS and other smoke products. Finally, the team tested different statistical and model-based approaches to estimate the impact of the observed smoke on surface PM_{2.5}.

TABLE OF CONTENTS

Executive Summary	4
1 Introduction.....	9
1.1 Background.....	9
1.2 Project Objectives.....	9
1.3 Study Spatial and Temporal Domain	9
1.4 Models Used in the Project.....	10
1.4.1 GAMS.....	10
1.5 Report Outline	10
2 Comparison of Different Methods for identifying Smoke Plumes from remote sensing imagery	11
2.1 Near-Real-Time (NRT) Smoke Detection Products over Texas	11
2.1.1 NOAA Hazard Mapping System (HMS) Fire and Smoke Product.....	11
2.1.2 GOES-R Aerosol Detection Smoke and Dust Product (GOES ADP).....	13
2.1.3 TROPOMI Ultraviolet Aerosol Index (UVAI).....	13
2.2 Additional Smoke-related metrics	15
2.2.1 IASI: CO and NH ₃ Total Column Amounts.....	15
2.2.2 OMI: AOD and Brown Carbon Estimates.....	15
2.2.3 GOES Aerosol Optical Depth (GOES AOD)	16
2.3 Critical Review of Methods to Identify Smoke Plumes in NRT	16
2.3.1 Smoke Flags (SF).....	16
2.3.2 Smoke Confidence Index (SCI).....	17
2.3.3 Figure of Merit in Space Analysis (FMS)	17
3 Investigating different remote sensing techniques to estimate the height and vertical profiles of smoke plumes	20
3.1 Using the MAIAC Plume Height/AOD relation to inform plume height estimates for higher confidence smoke pixels	20
4 Grand Merge Task 1 and Task 2 data set.....	21
4.1 Summary of Smoke Plume analysis from Tasks 1 and 2	22
4.2 Smoke Visualizer Tool	24
5 Investigating statistical methods to relate the smoke AOD observations to surface PM_{2.5} concentrations	26
6 Audits of Data Quality and Reconciliation with User Requirements.....	29
7 Conclusions	30
8 Recommendations for Further Study	31
9 References	32
Appendix A: Flowchart of processing code and output.....	37

List of Figures

FIGURE 1. EXAMPLE OF THE THREE NRT PRODUCTS ON 22 MAY 2020. (A) NOAA HMS SMOKE POLYGONS WITH DENSITY ESTIMATES; (B) GOES SMOKE SMOKE PIXELS CATEGORIZED BY DATA QUALITY; AND (C) TROPOMI UVAI FILTERED ACCORDING TO LIKELY SMOKE REGIME.....12

FIGURE 2. HOURLY FMS % FOR EXAMPLE DATE 17 APRIL 2020.....18

FIGURE 3. AOD GROUPED BY (LEFT) SCI AND (RIGHT) SF ACROSS ALL HOURS OF ALL 93 STUDY DAYS. IN THE CASE OF THE 89 PIXELS CATEGORIZED AS HIGH SCI, ONLY TWO INSTANCES WERE ASSOCIATED WITH NON-MISSING AOD. THE SCI=3 (AND SF = 20) RESULTS ARE THEREFORE PROVIDED FOR INFORMATION ONLY DUE TO INSUFFICIENT SAMPLE SIZE. WE LIST SAMPLE SIZE, N, WHERE SIGNIFICANTLY LESS THAN OTHERS.22

FIGURE 4. SMOKE-RELEVANT VARIABLES FOR ALL PIXELS IN STUDY DOMAIN GROUPED BY MONTH OF YEAR (JANUARY – JULY 2020). JULY IASI NH₃ AND CO DATA WERE NOT YET AVAILABLE AT THE TIME OF RAW DATA PROCESSING.....24

FIGURE 5. EXAMPLE GUI OUTPUT FOR DAILY SMOKE VISUALIZATION ON POTENTIAL SMOKE DATE OF APRIL 17, 2020.25

FIGURE 6. *MGCV::GAM.CHECK* PLOT OUTPUT FOR “CLIMATOLOGY” GAM OF HOUR OF DAY, MONTH, AND CITY ONLY.27

FIGURE 7. SMOOTH FUNCTIONAL FIT OF GOES AOD TO PM_{2.5} IN GAM. DASHED LINES ARE THE 1-SIGMA UNCERTAINTY OF THE FITS.....28

List of Tables

TABLE 1. TEMPORAL DOMAIN OF STUDY	10
TABLE 2. SMOKE FLAG VALUES AND THEIR INTERPRETATION.	16
TABLE 3. SMOKE CONFIDENCE INDEX VALUES AND THEIR INTERPRETATION.	17
TABLE 4. FMS (%) AGGREGATED ALL STUDY DATES. ONLY HOURS WITH NONZERO AGGREGATE OVERLAP ARE SHOWN. FOR GOES +HMS (HIGHEST SAMPLE SIZE) WE ADDITIONALLY PROVIDE FMS FOR THE MAIN BIOMASS BURNING PERIOD OF APRIL AND MAY.	19
TABLE 5. MAIAC-DERIVED PLUME HEIGHT ESTIMATES BASED ON GOES AOD IN SEVEN BINS.	20
TABLE 6. RELEVANT ANALYSIS VARIABLES IN GRAND MERGE DATASET.....	21
TABLE 7. AGGREGATED STATISTICS FOR SMOKE-RELEVANT VARIABLES (SPATIOTEMPORALLY AGGREGATED OVER.....	23

List of Acronyms

AAE – Absorption Ångstrom Exponent
AER – Atmospheric and Environmental Research
AOD – Aerosol Optical Depth
AAOD – Absorption Aerosol Optical Depth
AQRP – Air Quality Research Program
BB – Biomass Burning
BrC – Brown Carbon aerosol
CO – Carbon Monoxide
EAE – Extinction Ångstrom Exponent
EER – Exceptional Events Rule
EPA – Environmental Protection Agency
ESA – European Space Agency
FMS – Figure of Merit in Space
GASP – GOES Aerosol and Smoke Product (Retired)
GOES – Geostationary Operational Environmental Satellite
HYSPLIT – Hybrid Single Particle Lagrangian Integrated Trajectory Model
HMS – Hazard Mapping System
IASI – Infrared Atmospheric Sounding Interferometer
MAIAC – Multi-angle implementation of Atmospheric Correction
MetOp – Meteorological Operational Satellite
NAAQS – National Ambient Air Quality Standards
NetCDF – Network Common Data Form
NASA – National Aeronautics and Space Administration
NH₃ – Ammonia
NOAA – National Oceanic and Atmospheric Administration
NRT – Near Real Time
OMI – Ozone Monitoring Instrument
PM_{2.5} – Particulate Matter with diameter below 2.5 microns
ppb – parts per billion
QAPP – Quality Assurance Project Plan
TCEQ – Texas Commission on Environmental Quality
TROPOMI – Tropospheric Monitoring Experiment
UTC – Coordinated Universal Time
UVAI – Ultraviolet Aerosol Index

1 Introduction

1.1 Background

Biomass burning smoke can have major impacts on surface air quality both near the fires and hundreds of miles downwind. These smoke impacts pose two challenges for air quality managers. First, they want to accurately report the potential smoke impacts in time for the public to take protective actions. Second, they need to estimate the recent impacts of smoke on fine particulate matter (PM_{2.5}) to determine which elevated PM_{2.5} episodes may fall under the US EPA Exceptional Events Rule (EER). The EER determines the conditions under which the US EPA will forgo comparison of policy relevant air monitoring data to a relevant National Ambient Air Quality Standard (NAAQS).

Various satellite observations provide valuable information on the locations of fires and transport of smoke. Existing analysis products, such as the NOAA Hazard Mapping System (HMS) Fire and Smoke product, provide observed fire locations and identify regions that are being impacted by biomass burning smoke. However, there are multiple products that use different techniques to identify smoke plumes, and thus may disagree on the extent of the area covered by biomass burning smoke. In addition, due to the nature of these measurement systems, these products do not currently provide information on the height of the smoke plumes or estimates of the surface impacts of the observed smoke. An analysis of existing smoke products that increases our confidence in the identification of smoke and provides an estimate of smoke height and surface PM_{2.5} impact would greatly help TCEQ air quality managers protect the public and properly enforce air quality standards.

In this project, we evaluated the ability of three existing remote sensing products to accurately and consistently identify regions impacted by smoke. We compared and evaluated the smoke products using additional satellite observations that are sensitive to smoke, specifically observations of CO and NH₃ from IASI and aerosol optical depth (AOD) observations from GOES and OMI. We employed a method for estimating the height of the plumes detected by the HMS and other smoke products by using the relationship between remotely sensed plume height estimates and remotely-sensed AOD measurements. Finally, we tested different statistical and model-based approaches to estimate the impact of the observed smoke on surface PM_{2.5}.

1.2 Project Objectives

The objectives of this project are:

1. To compare different remotely sensed smoke identification products;
2. To investigate remote sensing techniques that estimate the height and vertical profiles of these smoke plumes; and
3. To investigate new statistical and machine learning methods to relate the smoke AOD observations to surface PM_{2.5} concentrations.

1.3 Study Spatial and Temporal Domain

Our study spatial domain was subset to the Texas/Gulf of Mexico region, with the following coordinate bounds: -120E, -80E, 10N, 40N

Our study temporal domain was subset to 93 days that, based on a manual review of NOAA HMS imagery, revealed possible smoke intrusions in the Texas region. The 93 dates are listed below, in YYYYMMDD format:

Table 1. Temporal domain of study

[1]	20200108	20200111	20200112	20200120	20200121
[6]	20200123	20200124	20200126	20200127	20200128
[11]	20200129	20200131	20200201	20200206	20200207
[16]	20200208	20200213	20200214	20200216	20200217
[21]	20200221	20200224	20200225	20200226	20200227
[26]	20200228	20200305	20200306	20200307	20200308
[31]	20200313	20200314	20200320	20200324	20200325
[36]	20200326	20200327	20200328	20200329	20200330
[41]	20200331	20200401	20200403	20200404	20200409
[46]	20200410	20200411	20200412	20200413	20200416
[51]	20200417	20200418	20200419	20200420	20200421
[56]	20200422	20200423	20200424	20200425	20200426
[61]	20200428	20200429	20200504	20200505	20200506
[66]	20200507	20200508	20200514	20200515	20200520
[71]	20200521	20200522	20200523	20200524	20200525
[76]	20200528	20200609	20200612	20200613	20200614
[81]	20200615	20200616	20200617	20200618	20200619
[86]	20200620	20200621	20200622	20200623	20200630
[91]	20200714	20200717	20200718		

1.4 Models Used in the Project

1.4.1 GAMS

Generalized additive models (GAMs) are a generalization of linear regression models that are able to account for the potentially non-linear dependence of the modeled variable on the values of the predictors. The functional dependence of each predictor is determined during the fit as a linear combination of basis functions, with a penalty applied for the number of degrees of freedom included in each functional form. Routines for training GAMs are included in the open-source R statistical program.

1.5 Report Outline

In Section 2, we provide the results from Task 1, where we compare different methods for identifying smoke plumes from remote sensing imagery. In Section 3, we present results from Task 2, where we explore vertical distributions of smoke plumes. In Section 4, we discuss the synthesis of Task 1 and 2 results into a single dataset. In Section 5 (Task 3), we demonstrate how the results from Tasks 1 and 2 can inform predictions of surface PM_{2.5} from smoke related AOD estimates. We conclude with key results and recommendations for future study.

2 Comparison of Different Methods for identifying Smoke Plumes from remote sensing imagery

In this task, we compared and evaluated three different NRT smoke detection products: NOAA HMS Fire and Smoke Product (HMS); GOES-R Smoke and Dust Product (GOES); and TROPOMI UV Aerosol Index (UVAI). These three products are described individually in Section 2.1. Our evaluation focused on dates in 2020 when fires were present within Texas, as well as instances where smoke is known to have been transported to Texas urban areas from fires in the rest of the US and/or Mexico (e.g., Wang and Talbot, 2017). Our comparisons used the figure of merit in space (FMS) evaluation metric, defined as the intersection over the union of the observed and calculated smoke plumes, which has been frequently used to evaluate smoke forecasts using satellite observations (e.g., Rolph et al., 2009; Stein et al., 2009). We note that the original project plan involved the use of the NOAA Automated Smoke Detection and Tracking Algorithm (ASDTA); however, as the ASDTA algorithm has been retired and replaced with the GOES product for the study time period of this project, the team selected the TROPOMI UVAI product to conserve the total amount of data sets being analyzed.

While simple comparisons of the three NRT products will allow us to assess their consistency, none of the products provide a “truth” dataset to use as a reference. (This also makes the training of machine learning algorithms to identify smoke difficult, as they require a truth dataset.) Thus, in this task we used additional satellite observations to determine if the detections of smoke from the three NRT products are robust. First, we used polar satellite observations of the trace gases CO and NH₃ from the Infrared Atmospheric Sounding Interferometer (IASI; on board the European Metop-A and B satellites) as an additional indicator of the presence of smoke. Both CO and NH₃ are emitted in large quantities by biomass burning (e.g., Akagi et al., 2011; Alvarado et al., 2011), and daily observations of NH₃ and CO (along with their ratio, e.g. Whitburn et al., 2017) from IASI was used to determine the extent of smoke transport.

Second, we used data from the polar-orbiting Ozone Monitoring Instrument (OMI) to identify areas that have large concentrations of brown carbon (BrC) aerosols, which are emitted by biomass burning. OMI provides absorption aerosol optical depth (AAOD) at five wavelengths between 342.5 nm and 483.5 nm once a day around 13:30 local solar time. The wavelengths can be used to calculate both AAE and EAE in the UV. High values of UV AAE imply the presence of BrC aerosols from biomass burning smoke: for example, Wang et al. (2016) found that AAE_{388/440} nm for BrC is generally ~4 worldwide, with a smaller value in Europe (< 2), compared to ~1 for black carbon aerosols from both biomass burning and anthropogenic sources. In addition, simultaneous calculations of EAE for the same wavelength window enable more accurate partitioning of AAE into biomass burning regimes. These OMI identifications of BrC aerosols are used to provide an additional, independent evaluation of the three NRT smoke products further described in Section 2.1.

2.1 Near-Real-Time (NRT) Smoke Detection Products over Texas

2.1.1 NOAA Hazard Mapping System (HMS) Fire and Smoke Product

To make the HMS Fire and Smoke product, National Environmental Satellite, Data, and Information Service (NESDIS) satellite analysts manually generate a daily operational list of fire locations and outline areas of smoke as polygons (Figure 1a). These analysts compare automated fire detections to the infrared satellite images used to produce them to

ensure each fire exists (Ruminski et al., 2006; Schroeder et al., 2008; Brey et al., 2018). Small fires are more difficult to detect and are underreported (e.g., Hu et al., 2016). False fire detections are removed, and fires that were not automatically detected are added manually.

Each polygon extent and density is determined by an analyst. After identifying fire locations, HMS analysts use imagery from multiple NOAA and NASA satellites to identify the geographic extent of smoke plumes (Rolph et al., 2009; Ruminski et al., 2006). Smoke detection is done primarily with visible-band geostationary GOES imagery, which has high temporal coverage (typically every 10 minutes), occasionally assisted by GOES infrared imagery and polar orbiting satellite imagery (Ruminski et al., 2006). Due to the frequent interference by cloud cover, the number and extent of smoke plumes reported in the HMS represents a conservative estimate. No information about the height or vertical profile of smoke plumes is provided.

Smoke density units are also provided, in micrograms per cubic meter ($\mu\text{g m}^{-3}$). The smoke density is categorized as light ($0\text{--}10 \mu\text{g m}^{-3}$), medium ($10\text{--}21 \mu\text{g m}^{-3}$), and heavy ($21\text{--}32 \mu\text{g m}^{-3}$) smoke. The smoke densities are provided as a very rough guide, as they remain from the old GOES Aerosol and Smoke Product (GASP) which has since been replaced with GOES-16 and 17. Due to their highly uncertain and qualitative nature, we have eliminated the smoke density grades in our final datasets and simply designated HMS with a binary “smoke/no smoke” flag.

Data Access and Download. Smoke polygon shapefiles were accessed from <https://www.ospo.noaa.gov/Products/land/hms.html>. Smoke data are available beginning 5 August 2015.

Data Processing. The HMS polygons (variable resolution) are converted to pixels on the native GOES grid (2km). Each polygon has associated timing (UTC), density, and polygon geometry. The daily HMS shapefile is split into hourly polygons based on the polygons' starting and ending times. The time coverages of the polygons must enclose a given hour. The GOES pixels encompassed in the hourly HMS polygons are then matched. As part of intermediate processing, the polygons' associated density values are also assigned to these GOES pixels. If multiple polygons cover the same pixels in an hour, the midpoint of the

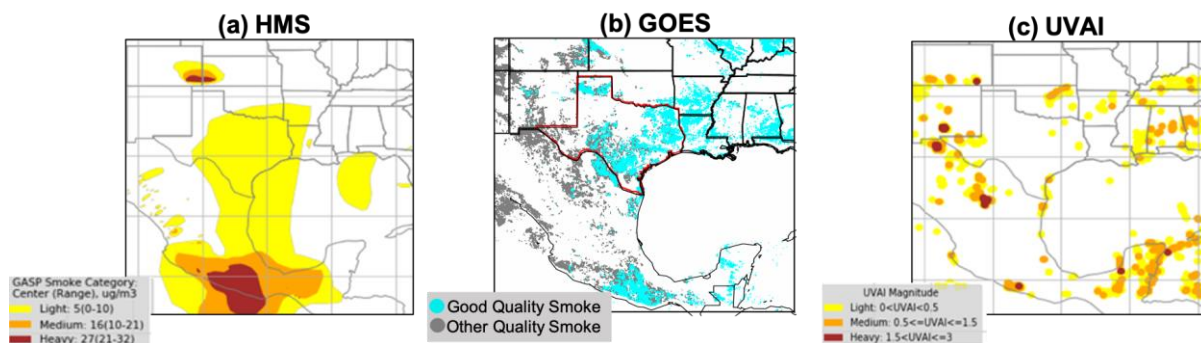


Figure 1. Example of the three NRT products on 22 May 2020. (a) NOAA HMS Smoke Polygons with density estimates; (b) GOES Smoke Smoke Pixels categorized by data quality; and (c) TROPOMI UVAI filtered according to likely smoke regime.

range of the highest reported density value is used (i.e., 5=low, 16=medium, 27=high). As noted previously, however, the density information has been eliminated from the final data set. See Appendix A for additional details.

2.1.2 GOES-R Aerosol Detection Smoke and Dust Product (GOES ADP)

We are using the GOES-R L2+ CONUS products in the current analysis. For details about the GOES-R products, please refer to the users' guide (GOES-R Users' Guide, 2019). The data is download from the [AWS S3 Explorer \(noaa-goes16.s3.amazonaws.com\)](https://noaa-goes16.s3.amazonaws.com).

The GOES ADP aerosol detection algorithm detects smoke and dust contaminated pixels using images taken by the Advanced Baseline Imager (ABI) flown on the GOES-R series NOAA operational geostationary meteorological satellites (NOAA/NESDIS/STAR, 2018). The algorithm provides an initial estimate of the presence or absence of smoke or dust within each ABI pixel in 10-minute swaths. The smoke and dust detection algorithm is based on the fact that smoke/dust exhibits features of spectral dependence and contrast over both the visible and infrared spectrum that are different from clouds, surface, and clear-sky atmosphere (NOAA/NESDIS/STAR, 2018). The GOES ADP smoke and dust algorithm has been tested for different scenarios such as wildfires and dust storms against MODIS and CALIPSO observations. In this study, we only use GOES ADP smoke pixels that are flagged as good quality (Figure 1b). The 2km native GOES ADP grid is the common grid on which all other products are placed, typically using nearest neighbor regridding. The GOES ADP image collects data in 10-minute swaths (6 files in an hour). The ADP consists of three flags for each pixel in the image indicating the presence of aerosol and whether the type of aerosol is dust or smoke. Data is produced under conditions of clear sky, snow-free, and geolocated source data to local zenith angles of 90 degrees and to solar zenith angles of 87 degrees.

Data Access and Download. NetCDF4 files for the study dates were downloaded from Amazon Web Services S3 Explorer (noaa-goes16.s3.amazonaws.com). The data is stored by day of year, with convention of January 1 set to day "001". There is an automated download script, but also the option to download the required dates manually. As the file collection can quickly get very large, for the average user it is recommended that the individual dates and times are downloaded as needed from the AWS portal rather than in bulk. See Appendix A for additional details.

Data Processing. We use the smoke product of the ADP and its data quality flags (DQF) where the GOES ADP smoke is classified into three levels (good, medium, and low). We only use the smoke with good data quality in our analysis. The variables of smoke and DQF are then read in from each 10-minute resolution file and are used to create an hourly average smoke mask, where a pixel is classified as smoke for a given hour if there was good quality smoke at that location in more than 50% of the files (>3 files) for that hour.

2.1.3 TROPOMI Ultraviolet Aerosol Index (UVAI)

The ultraviolet aerosol index (UVAI) observations from the European TROPOMI instrument replaced ASDTA to conserve the total amount of smoke datasets being

examined. Figures in the official TROPOMI documentation¹ suggest smoke for UVAI values ≤ 3 . This threshold is justified further by Vadrevu et al., 2015 who find that agricultural fire UVAI (focus region: Asia) is on the lower end of the UVAI signal (0.5-2.5) versus other fire types (1-3). We use the Vadrevu et al. (2015) biomass burning UVAI thresholds to establish a selection window for smoke-impacted pixels in our study domain ($0 < \text{UVAI} \leq 3$; Figure 1c). As discussed in Vadrevu et al. (2015), however, the UVAI associated with agricultural biomass burning is likely a smaller magnitude signal with weaker correlation than those associated with forest- or peat-type fires. Given the prevalence of agricultural smoke in the Texas region during the April/May peak smoke months, it is possible that UVAI is a weaker correlate for smoke activity represented by the Texas/Gulf of Mexico study region.

Data Access and Download. Data was downloaded from a NASA data portal: https://disc.gsfc.nasa.gov/datasets/S5P_L2_AER_AI_HiR_1/summary using the following steps:

The "Subset/Get Data" Option was used, with options modified as below:

- Download Method: Get File Subsets using the GES DISC Subsetter
- Date range: 2020-01-01 to 2020-07-25
- Bounding box: -109.1,16.4,-82.9,37.8
- Variables: aerosol_index_354_388; aerosol_index_354_388_precision; qa_value (data quality value); time_utc (Time of observation as ISO 8601 date-time string)
- Data Presentation: CROP

Selecting "Get Data" will bring you to a window with all the generated files. Download the text file, and follow the wget instructions for downloading multiple data files at once. Make sure your txt file with each file name is executable. Ultimately, you should have a *.netrc* file and a *.urs_cookies* file in your home directory that will then allow you to execute this command on your download file and download the associated file content.

For example:
`wget --load-cookies ~/.urs_cookies --save-cookies ~/.urs_cookies --auth-no-challenge=on
--keep-session-cookies --content-disposition -i
<subset_S5P_L2_AER_AI_HiR_1_20201001_153753.txt>`

Data Processing. Currently our UVAI smoke flag is binary: we flag smoke if $0 < \text{UVAI} \leq 3$, based on results from Vadrevu et al. (2015). We then regrid the UVAI data set to the GOES grid using nearest neighbor regridding. See Appendix A for additional details.

¹ <https://earth.esa.int/documents/247904/2474726/Sentinel-5P-Level-2-Product-User-Manual-Aerosol-Index-product>

2.2 Additional Smoke-related metrics

2.2.1 IASI: CO and NH₃ Total Column Amounts

Both CO and NH₃ are emitted in large quantities by biomass burning and daily observations of NH₃ and CO from IASI can be used to determine the extent of smoke transport while providing an independent observational check on the three smoke NRT smoke products described in Section 2.1.

IASI provides total column amounts (molecules cm⁻²) of CO and NH₃ twice daily at approximately 0.4° × 0.5° resolution.

Data Access and Download. IASI Data can be accessed from the IASI data portal at https://iasi.aeris-data.fr/NH3_IASI_B_data/ (for NH₃) and https://iasi.aeris-data.fr/co_ac_saf_iasi_b_arch/ (for CO). However, the individual files are very large (1GB) and the download has been automated file-by-file for each date as needed. See Appendix A for additional details.

Data Processing. A temporary .nc file is downloaded, subset to the study domain of interest, and then deleted. The subset data is saved as a .csv file for that day for each of NH₃ and CO. These csv files are then regridded in R to a common grid and saved to an aggregated csv files for all dates of interest in the study time. The python script “NH3_CO.ipynb” downloads each file for the temporal domain, subsets them to the spatial domain, writes a csv file for each of the dates (one each for CO and NH₃) and then deletes the original 1GB netcdf file. The R file “regrid_iasi_nh3_co.r” ingests all the csv files, regrids them to a common destination grid (the NH₃ grid) and writes out an aggregated csv file for all dates. In addition, a series of QC figures for the checking the regridding process is also written out. Note that as of Dec 6, 2020, IASI did not provide public access to NH₃ and CO from July 2020. Currently, the NH₃ and CO dates go through June 2020 (and therefore last 3 of the 93 dates in July are excluded at this time).

2.2.2 OMI: AOD and Brown Carbon Estimates

The OMI Brown Carbon processor was developed for TCEQ in 2020 (Alvarado & Dayalu 2021). The processor uses AAOD and AOD data from OMI to calculate AAE and EAE, respectively. The ratio of these quantities in turn provides a proxy for Brown Carbon (BrC) content of the local atmosphere and, therefore, smoke influence.

Data Access and Download. 48h 1°×1° AAOD and AOD was downloaded from the NASA Giovanni portal (<https://giovanni.gsfc.nasa.gov/giovanni/>). The Brown Carbon processor has been extensively documented as part of the associated TCEQ 2020 Work Order. A Users’ Guide and Technical Memo exist for both download of required data sets and running and interpretation of processor results (Alvarado & Dayalu 2020). All required datasets for the 93-day subset were downloaded according to instructions in the Users’ Guide.

Data Processing. The processor was run for the 93-day subset. The final clustering of smoke pixels incorporated days from the previous run of the processor (99 days) resulting in a total clustering dataset of 192 days. The final data set includes AAE,

EAE, coordinate information, and a three-way *k-means* clustering assignment for the AAE/EAE ratio namely: 1 (possible BrC mixtures); 2 (possible dust); and 3 (possible BrC dominant).

2.2.3 GOES Aerosol Optical Depth (GOES AOD)

The GOES AOD data is collected in 5-minute swaths (12 files in an hour). The AOD product is collected at 550nm and consists of pixels containing a dimensionless quantity representing the atmospheric absorption optical thickness due to ambient aerosol. The product is derived from ABI reflectance measurements through physical retrievals that utilize a lookup table of top of the atmosphere reflectance that is calculated from a radiative transfer model. The product is reported at 0.55 μm . The data is produced under conditions of clear sky, snow-free, geolocated source data to local zenith angles of 90 degrees, to solar zenith angles of 90 degrees, and surface with reflectance not greater than 0.25 (GOES-R Users' Guide). Similar to the GOES ADP, the GOES AOD are classified into three levels by their retrieval qualities of good, medium, and low. We only use the AOD with good data quality in the current analysis.

Data Access and Download. See Section 2.1.2 for AWS download instructions.

Data Processing. We use the AOD and its data quality flags (DQF) where the GOES AOD is classified into three levels (good, medium, and low). We only use the smoke with good data quality in our analysis. The variables of smoke and DQF are then read in from each 5-minute resolution file and are used to calculate an hourly average AOD. If a pixel has good quality AOD for a given hour in more than 75% of the files (>9 files), the AOD reported is the average among all valid files for that hour. Otherwise, the hourly average AOD for that pixel is set to missing.

2.3 Critical Review of Methods to Identify Smoke Plumes in NRT

2.3.1 Smoke Flags (SF)

Table 2. Smoke Flag values and their interpretation.

Smoke Flag Value	Interpretation
1	No overlap; HMS only
2	No overlap; GOES only
3	No overlap; UVAI only
11	HMS + GOES overlap
12	GOES + UVAI overlap
13	HMS + UVAI overlap
20	HMS+GOES+UVAI all overlap

We used the HMS, GOES, and UVAI smoke products on the GOES 2km native grid to establish a SF system to inform both a simple Smoke Confidence Index (SCI) and the Figure of Merit in Space (FMS) calculations (described in Sections 2.3.2 and 2.3.3, respectively). For any given pixel at any given UTC hour, an SF is provided as shown in Table 1. We note that smoke flags imply that there is at least one NRT product that exhibits smoke presence; to save data processing time and storage space, we eliminated the need to provide a smoke flag value of “00” (i.e., no smoke in any product). In other words, if a coordinate only exists in the final data set if there was smoke identified for that location, date and time by least one NRT smoke product.

2.3.2 Smoke Confidence Index (SCI)

The SCI provides a simple, distilled version of the SF system in that overlap among the three NRT smoke products suggests higher confidence that a given pixel is impacted by smoke. Table 2 lists SCI values and their interpretation.

Table 3. Smoke Confidence Index values and their interpretation.

Smoke Confidence Index	Interpretation
1	Low confidence (SF = 1, 2, or 3; no overlap)
2	Medium confidence (SF = 11, 12, or 13; two products overlap)
3	High confidence (SF = 20; three products overlap)

2.3.3 Figure of Merit in Space Analysis (FMS)

The SF system also enables a Figure of Merit in Space (FMS) calculation. The purpose of the temporal FMS analysis is to (1) assess the performance of the varying smoke products during times of known and more intense smoke activity (April and May seasonal Mexico/Yucatán agricultural fires) versus other times of the year, and (2) by time of day, to account for greater coverage by certain products at particular times of day.

Since all data from all products reflect varying time slices, FMS analyses provide most information when conducted for overlapping hours rather than for a day as a whole. For any given hour, the FMS is calculated as the number of pixels that overlap relative to the total number of smoke pixels identified for each (i.e., the intersecting smoke pixels divided by the union of the respective NRT smoke pixels). Equation 1 below shows an example calculation for the FMS % of GOES and HMS overlap for a hypothetical day at hour hh .

$$FMS_{t=hh} = 100 \times \frac{\sum SF_{11}}{\sum (SF_1, SF_2, SF_{11}, SF_{20})} \quad \text{Eq 1}$$

As shown in Equation 1, the %FMS for overlapping GOES and HMS smoke pixels involves using the relevant SF quantity which contains information on pixel overlap. In this case, the union is obtained by counting all pixels for that day and hour that have an SF value of “11” (see Table 2) and dividing by the sum of all pixels that are designated as smoke by GOES and/or HMS (ie., $SF \in [1,2,11,20]$; see Table 2)

We conducted FMS analyses over the entire study time period. Because measurement hours differed across smoke products, our FMS analyses were conducted each hour of each day; aggregated hourly over the 93 days; and aggregated across all days and hours (Table 4). All FMS results have been tabulated, with daily FMS results by hour additionally saved to the figure archive and displayed in the GUI. Figure 2 displays a sample figure of daily FMS broken down by hour.

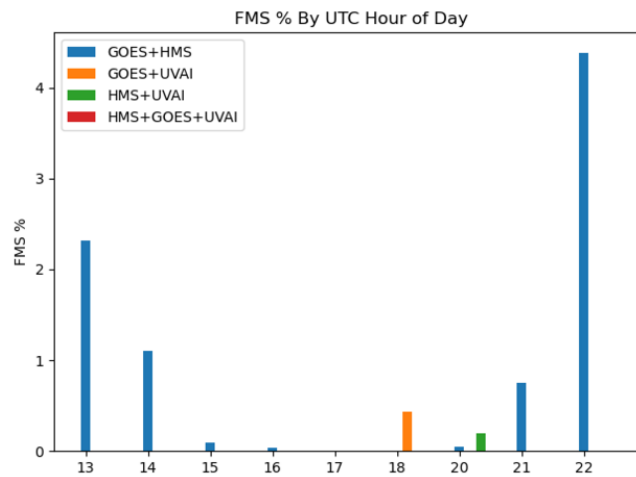


Figure 2. Hourly FMS % for example date 17 April 2020.

Table 4. FMS (%) aggregated all study dates. Only hours with nonzero aggregate overlap are shown. For GOES +HMS (highest sample size) we additionally provide FMS for the main biomass burning period of April and May.

Time window	GOES+HMS	GOES+UVAI	HMS+UVAI	HMS+GOES+UVAI
13 UTC	1.0	0	0	0
14 UTC	0.5	0	0	0
15 UTC	0.1	0	0	0
16 UTC	0.1	0	0	0
17 UTC	0.1	0	0	0
18 UTC	0.1	0.1	0.1	0
19 UTC	0.1	0.3	0.1	0
20 UTC	0.4	0.2	0.1	0
21 UTC	1.4	0	0	0
22 UTC	2.1	0	0	0
23 UTC	0.7	0	0	0
ALL DAYS	0.7	0.06	0.01	0
<i>Apr/May</i>	0.9			

On the sample date in Figure 2, FMS calculated across the entire day for GOES+HMS overlap was 0.8%, but we see from the hourly breakdown that the peak was significantly higher (>4%) at hour 22, with additional peaks >1% over the course of the day. Therefore, without the hourly break down, the true FMS metric would be significantly underestimated if we aggregated across all hours. That is, the large number of pixels across all hours would create a large union denominator that would obscure a relevant intersection.

A basic FMS calculation across all dates indicates low overlap among products (Table 4). The highest overlap is 0.7% for $(GOES \cap HMS) / (GOES \cup HMS)$; product intersections with TROPOMI UVAI are much less, primarily due to less temporal coverage of the TROPOMI product. For comparison, we calculated the overlap between GOES and HMS for the peak April/May biomass burning season, the $(GOES \cap HMS) / (GOES \cup HMS)$ is still low (0.9%) but is a 30% increase relative to the full 93 day data set.

3 Investigating different remote sensing techniques to estimate the height and vertical profiles of smoke plumes

3.1 Using the MAIAC Plume Height/AOD relation to inform plume height estimates for higher confidence smoke pixels

We used a recently published relationship between smoke plume height estimated by the NASA MODIS MAIAC algorithm and thickness of aerosols in the atmosphere (Cheeseman et al., 2020). We used GOES aerosol thickness estimates to calculate a GOES AOD-based estimate of plume height (Table 5). The plume height variable is included in the grand merge dataset described in the Task 1 section above. In addition, Table 5 provides a reference for quantiles associated with the mean plume height in each AOD bin.

Cheeseman et al. (2020) showed that, for binned AOD values, $PH = 527 * AOD$ ($R^2=0.97$). The relation was found to hold specifically for binned AOD; the relation was not significant for collocated AOD and PH values. Similarly, we created seven bins for our GOES AOD. We calculated PH for each bin's mean AOD using the Cheeseman et al. (2020) relation. Table 5 summarizes the statistics for this analysis, conducted for AOD values across all 93 days.

These plume height values can be informative when combined with higher confidence smoke pixels.

Table 5. MAIAC-derived plume height estimates based on GOES AOD in seven bins.

	AOD_Mean	AOD_0.25_quartile	AOD_0.75_quartile	PH_m_Mean	PH_m_25qtl	PH_m_75qtl
0	0.257203	0.167063	0.335839	135.546201	88.041999	176.987375
1	0.655576	0.562088	0.737476	345.488728	296.220157	388.649942
2	1.052560	0.957367	1.134489	554.699110	504.532316	597.875860
3	1.507726	1.386284	1.617843	794.571830	730.571556	852.603452
4	1.989615	1.870721	2.093578	1048.526914	985.869748	1103.315682
5	2.455782	2.363600	2.534734	1294.197122	1245.617145	1335.804711
6	3.423601	2.852407	3.496252	1804.237609	1503.218572	1842.524705

4 Grand Merge Task 1 and Task 2 data set

We created daily smoke “grand merge” data files where all relevant data from Tasks 1 and 2.1 are gridded to the same coordinates. The daily “grand merge” data are standalone datasets that form the basis for all subsequent tasks and analyses. We used the grand merge dataset to create a smoke visualizer tool, and an archive of figures and tables for the entire 93-day aggregate analysis as well as for individual days. We also used the grand merge data set to conduct a detailed Figure-of-Merit in space analysis where we output smoke product overlap (i) across all 93 days; (ii) broken down by hour across all 93 days; (iii) daily; (iv) daily by hour. Table 6 summarizes the key variables in the grand merge data set. Due to file size, the grand merge data is output for each day with a file naming convention of `sci_iasi_omi_grand_merge_<YYYYMMDD>.csv`. The grand merge data forms the basis for Task 3, where we examine the ability of our smoke product (including AOD and the value of the SCI) to predict surface PM_{2.5} concentrations.

Table 6. Relevant analysis variables in Grand Merge dataset.

Variable	Description
Lon	Longitude, degrees E (range: -120E to -80E)
Lat	Latitude, degrees N (range: 10N to 40N)
Date (YYYYMMDD)	Year, Month, and Day of measurement
Time (UTC)	Time of Measurement (UTC), rounded to hourly
Smoke Flag	01=No overlap; HMS only 02=No overlap; GOES only 03=No overlap; UVAI only 11=HMS+GOES overlap 12=GOES+UVAI overlap 13=UVAI+HMS overlap 20=3-way overlap
Smoke Confidence Index	Flag of 0X = 1 (low) Flag of 1X = 2 (med) Flag of 20 = 3 (high)
GOES AOD	Aerosol Optical Depth from GOES
Mean_PlumeHeight_m	Plume Height Estimated from GOES AOD and MAIAC
NH3_CO_ratio	Ratio of total columns. Note that only total column measurements that are proximal in time have their ratios calculated. The threshold for temporal proximity is ± 3000 sec (± 49 minutes). The value is set to NA otherwise.
CO Total Column	Total column CO (molec cm ⁻²)
OMI BrC Cluster ID	1= potential smoke mixtures, 2= non-smoke, 3=heavy smoke
OMI AAE	Absorption Ångstrom Exponent
OMI EAE	Extinction Ångstrom Exponent

For future plume analysis, we also subset the very large “grand merge” dataset to a single file containing a significantly narrowed-down list of locations and times for pixels corresponding to (i) medium and high Smoke Confidence Index (SCI) values, and (ii) “Brown Carbon Dominant”. The data subset only includes instances for which GOES aerosol optical

depth (AOD) measurements and, therefore, Plume Height estimates are available. The subset incorporates all relevant auxiliary variables including NH_3/CO ratio, CO Total Column, and BrC cluster ID. The subset contains 78,783 coordinate pairs over 38 days; as expected, the majority of the 38 days (33/38) falls in the April/May peak Yucatán biomass burning season.

4.1 Summary of Smoke Plume analysis from Tasks 1 and 2

Our hypothesis was that higher values of the SCI correspond to significantly higher values of AOD. Our analysis confirmed our hypothesis, suggesting value in assessing smoke impacts by evaluating multi-smoke product overlap (Figure 3). Specifically, AOD values corresponding to a medium or high SCI were on average over three times greater than those with a low SCI (Figure 3, left panel). However, given the overpass time restrictions of the TROPOMI UVAI product, SCIs of 3 (i.e., high SCI) were rare, and was more a reflection of sample time mismatches from the TROPOMI UVAI product rather than ubiquitous spatial mismatching. Furthermore, of the 89 pixels that were identified with an SCI of 3, only two instances had a corresponding AOD value; the remaining instances had AOD values that were masked either through insufficient data quality or missing for other reasons. We also break down the AOD by Smoke Flag (SF) that provides more resolved information on overlap of specific products (Figure 3, right panel). Based on AOD binning alone, we note that the GOES smoke product generally correlates with higher AOD than either HMS or UVAI alone. GOES+HMS overlap in turn correlates to higher AOD than GOES alone, but the statistical significance of this needs to be assessed. We also note that given the relatively low sample size of TROPOMI when compared to GOES and HMS, the medium SCI values are biased toward GOES+HMS overlap (Figure 3).

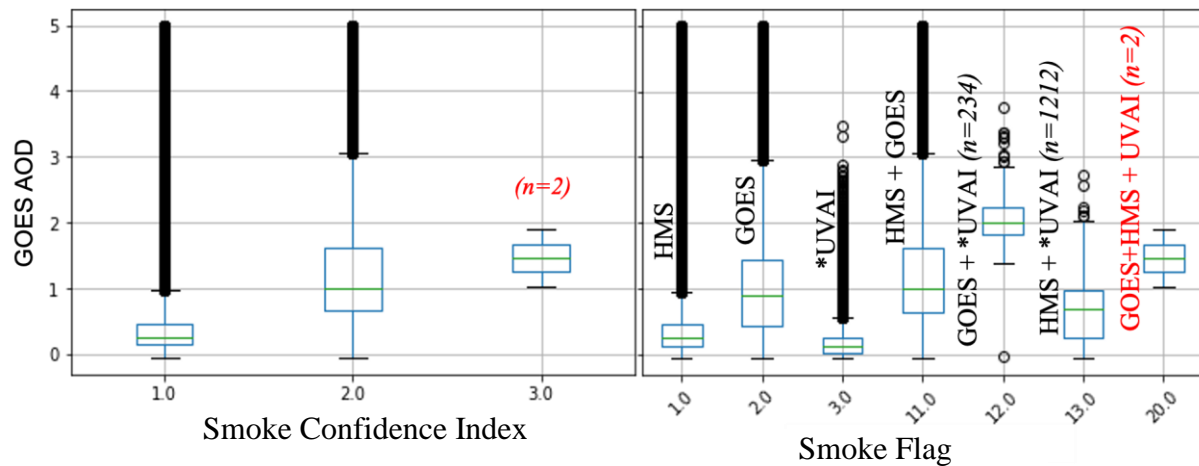


Figure 3. AOD grouped by (left) SCI and (right) SF across all hours of all 93 study days. In the case of the 89 pixels categorized as high SCI, only two instances were associated with non-missing AOD. The SCI=3 (and SF = 20) results are therefore provided for information only due to insufficient sample size. We list sample size, n, where significantly less than others.

Table 7 summarizes the aggregate statistics of relevant variables over the full 93-day period, for each SCI, Brown Carbon (BrC), and smoke flag (SF) category. Overall, we find that BrC dominant and/or high SCI values are associated with higher means and quantiles of smoke-relevant variables. In general, we see that pixels only identified as smoke by GOES (SF = 2) were consistently associated with higher statistics of smoke-relevant variables suggesting higher confidence in GOES smoke identification algorithm. We note that due to different overpass times and measurement frequencies, high SCI (value of 3) instances were rare and occurred only 89 times over the entire 93-day subset. However, while the small sample size prevents us from drawing any significant conclusions from the SCI=3 category, we provide the results for reference. We further note that due to the higher sample size of GOES and HMS, the SCI=2 values are biased toward the GOES+HMS smoke flag of 11.

As an additional independent check, we found that the median BrC cluster associated with an SCI of 2 (and SF of 11 or 12) was “BrC Dominant”, providing further confidence in both our smoke index and brown carbon algorithm. For all other SCI and SF categories the median BrC cluster was the very broad “BrC mixtures” category. The associated mean Absorption:Extinction Ångstrom Exponent ratio (AAE/EAE) used to derive BrC content associated with “BrC Dominant” is 3.4 (25th, 75th quantiles: 3.2, 3.6) (Table 7).

Table 7. Aggregated statistics for smoke-relevant variables (spatiotemporally aggregated over

	Mean GOES AOD (Quantiles 25, 75)	Mean IASI NH ₃ /CO (Quantiles 25,75)	Mean IASI CO (Quantiles 25, 75)	Mean OMI AAE/EAE (Quantiles 25, 75)
SCI=1(Low)	0.35 (0.15, 0.48)	0.005 (0.002, 0.006)	2.6 (2.1, 3.0)E+018	2.2 (1.7, 2.7)
SCI=2(Med)	1.2 (0.66, 1.6)	0.008 (0.004, 0.011)	3.9 (2.6, 4.7)E+018	3.0 (2.0, 3.6)
SCI=3(High)	1.5 (1.3, 1.7) * <i>n</i> =2	0.005 (0.002, 0.007)	3.1 (1.7, 3.8)E+018	2.3 (1.7, 2.5)
BrC Mix	0.23 (0.09, 0.31)	0.004 (0.002, 0.006)	2.6 (2.1, 3.0)E+018	1.8 (1.7, 1.7)
Other Aerosol	0.16 (0.06, 0.22)	0.003 (0.001, 0.004)	3.9 (2.6, 4.7)E+018	3.3 (2.5, 4.1)
BrC Dominant	0.58 (0.23, 0.80)	0.007 (0.003, 0.009)	3.1 (1.7, 3.8)E+018	3.4 (3.2, 3.6)
SF =1 (HMS)	0.35 (0.14, 0.47)	0.005 (0.002, 0.006)	2.6 (2.1, 3.0)E+018	2.2 (1.7, 2.7)
SF =2 (GOES)	1.0 (0.43, 1.4)	0.006 (0.002, 0.009)	3.9 (2.6, 4.7)E+018	2.6 (1.7, 3.5)
SF = 3 (UVAI)	0.22 (0.04, 0.25)	0.003 (0.001, 0.004)	3.1 (1.7, 3.8)E+018	2.9 (1.7, 3.9)
SF =11 (H+G)	1.2 (0.66, 1.6)	0.008 (0.004, 0.011)	2.6 (2.1, 3.0)E+018	3.0 (2.0, 3.6)
SF = 12 (G+U)	2.1 (1.8, 2.3)	0.013 (0.010, 0.016)	3.9 (2.6, 4.7)E+018	3.4 (3.5, 3.6)
SF = 13 (H+U)	0.65 (0.27, 0.99)	0.006 (0.003, 0.008)	3.1 (1.7, 3.8)E+018	2.7 (1.8, 3.4)

We also conducted an analysis by month of year to evaluate any seasonal patterns; these results are shown in Figure 4. While all 93 dates were selected as potential smoke-heavy dates

Figure 4 shows that (as expected) all smoke-relevant variables for the region peak in the April/May Yucatán/Mexico biomass burning period.

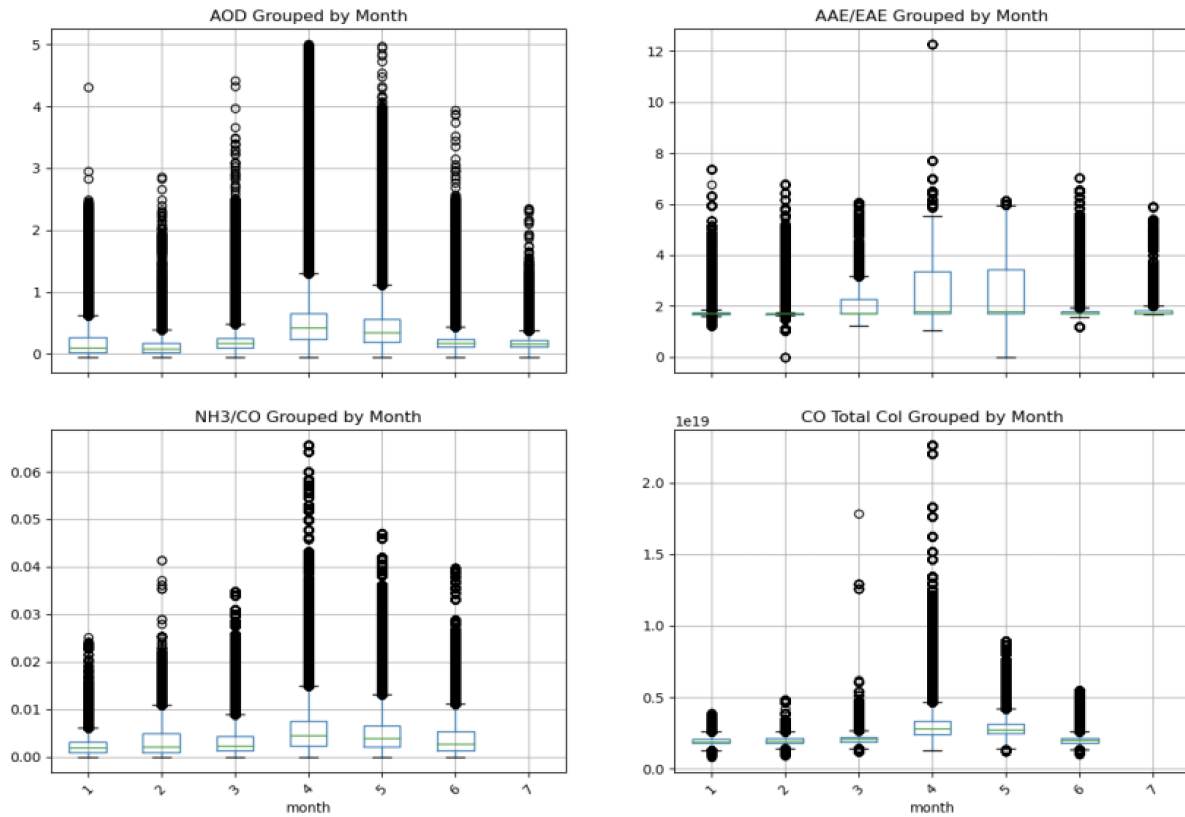


Figure 4. Smoke-relevant variables for all pixels in study domain grouped by month of year (January – July 2020). July IASI NH₃ and CO data were not yet available at the time of raw data processing.

4.2 Smoke Visualizer Tool

For a quick-look of output for each study date, we created a smoke Graphical User Interface (GUI) in python, which uses the original grand merge data as input. The tool enables the user to select a date from a calendar and scroll through/zoom in/save daily plots. We chose not to include an aggregate statistics option, as creating those images from the entire grand merge data set is computationally intensive and impractical for this simple GUI. The figures and tables for the aggregate data set are available in the static figure archive. While the daily plots are also available in the static figure archive, the GUI provides an additional user-friendly option for quick access to daily figures. Figure output from the GUI includes maps of SCI, SF, NH₃/CO, CO, BrC, AOD, Plume Height, and daily FMS broken down by hour (**Figure 5**).

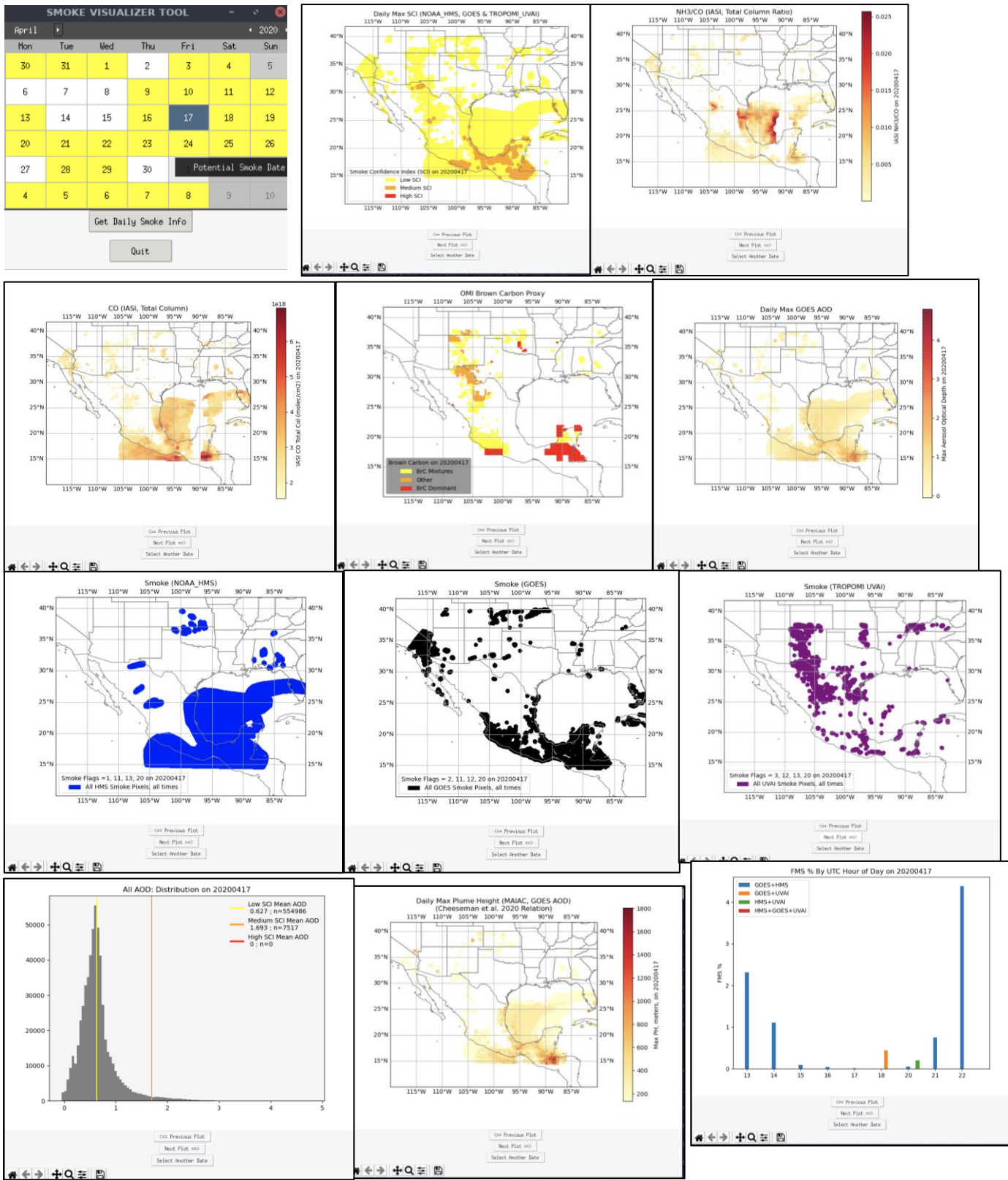


Figure 5. Example GUI Output for Daily Smoke Visualization on potential smoke date of April 17, 2020.

5 Investigating statistical methods to relate the smoke AOD observations to surface PM_{2.5} concentrations

Several studies have successfully converted satellite AOD to ground-level PM_{2.5} estimates using statistical techniques, CTM-based approaches, or hybrid approaches, generally for continental to global spatial scales and monthly to annual time scales. Statistical approaches train statistical models, such as non-linear generalized additive models (GAMs; Strawa *et al.*, 2013; Sorek-Hamer *et al.*, 2013), on historical ground level monitoring (GLM) data to predict ground-level PM_{2.5} using satellite AOD measurements and other meteorological and geographic data. CTM-based approaches use computer models of air quality, called “chemical transport models”, to determine a time-varying relationship between ground-level PM_{2.5} concentrations and satellite AOD measurements. This relationship is then used to scale the CTM aerosol profile until the CTM-calculated AOD matches the satellite AOD measurement, providing a better estimate of the ground-level PM_{2.5} concentration than would be possible from the CTM alone. Hybrid methods combine statistical and CTM-based approaches by training a statistical model to correct the errors in the initial CTM-based satellite estimates of the ground-level PM_{2.5} concentrations. For example, recent work has used a hybrid approach where CTM-based approaches are followed by a second step that uses geographically weighted regression (GWR) to correct for errors in the first-step estimates (van Donkelaar *et al.*, 2015b). These corrections require long-term (multiple years), reliable GLM data over a large region, including both urban and rural sites.

Statistical approaches (*e.g.*, Sorek-Hamer *et al.*, 2013, 2015; Strawa *et al.*, 2013) can be more accurate if sufficient GLM data is available for the training, but the CTM-based approaches (*e.g.*, van Donkelaar *et al.*, 2006, 2010, 2011, 2015a; Geng *et al.*, 2015) are required in areas with either no GLM data or GLM data of unreliable quality.

Here we investigated whether the GOES AOD data (Section 2.2.3) during smoky period (smoke confidence index > 0, see Section 2.3.2) could be used in a statistical (GAM) model to help predict ground-level PM_{2.5} concentrations. We used the *mcgv* package in the R software to perform the statistical fits. The input data was assembled from TCEQ hourly PM_{2.5} monitoring data for January to June 2020 for El Paso, Houston-Galveston-Brazoria, Dallas-Fort Worth, San Antonio, and Austin. The data was collected for us from the Texas Air Monitoring Information System (TAMIS) by Erik Gribbin of TCEQ. We then found the nearest valid GOES AOD observation in space and time to the hourly PM_{2.5} data for analysis, along with the nearest OMI AAE/EAE and IASI CO and NH₃ columns. This matching left over 5000 individual hourly PM_{2.5} observations for fitting. Most of the points had a smoke confidence index of 1, with only one point having a value of 2. Most points were in OMI BrC cluster 1, with about 200 points being cluster 2 and about 50 cluster 3.

Unfortunately, the satellite observations generally had a low correlation with surface PM_{2.5}. GOES AOD only had a correlation of $r = 0.17$ with the hourly surface PM_{2.5}. The correlations for other satellite variables were generally lower (CO column, $r = 0.09$; OMI AAE, $r = 0.05$; NH₃/CO ratio, $r = 0.01$; OMI EAE, $r = -0.02$). This suggests that the satellite observations will provide little ability to determine hourly surface PM_{2.5} during potentially smoky periods.

We further examined the ability of the AOD observations to determine surface PM_{2.5} by fitting GAMs of the form:

$$g(\mu_i) = \beta_0 + f_1(x_{i,1}) + \dots + f_n(x_{i,n}) + f_p(H_i) + M + C$$

where μ_i is the i th hour's $\text{PM}_{2.5}$ observation, $g(\mu_i)$ is the “link” function (here, a log link is used), $x_{i,j}$ are the satellite predictors fit, with the corresponding $f_j(x_{i,j})$ being a (initially unknown) smooth function of $x_{i,j}$ made from a cubic-spline basis set with 6 knots. Three non-satellite predictors are also included to establish a climatology: a smooth periodic function $f_p(H_i)$ of the hour of day (H_i); a factor for the month M ; and a factor for the observation city C . To reduce the possibility of over-fitting the data, we set the “gamma” parameter to 1.4 for these fits, as recommended by Wood (2006).

Including no satellite observations (*i.e.*, only including H_i , M , and C as climatological predictors) shows all three of these climatological variables as significant, but gives an adjusted R^2 of only 0.32, suggesting a poor fit that only explains 32% of the variance. While the residuals show no trend with fitted value, the residuals differ from a normal distribution significantly along the high tail, also indicating a poor fit (**Figure 6**).

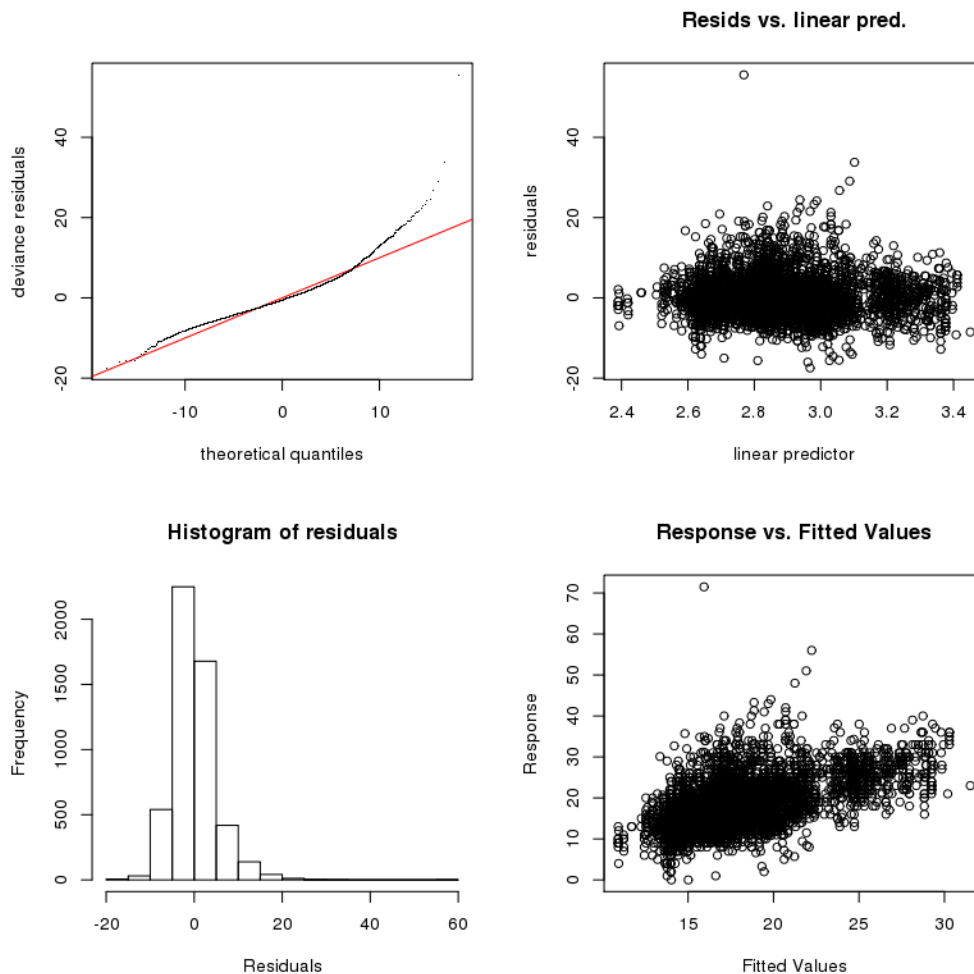


Figure 6. `mgcv::gam.check` plot output for “climatology” GAM of hour of day, month, and city only.

Unfortunately, adding in the GOES AOD and other satellite observations does not significantly improve the ability to predict surface $\text{PM}_{2.5}$. While GOES AOD is a significant predictor

($p < 0.001$), it does not increase the variance explained by the GAM model much (adj. R^2 of 0.34 instead of 0.32 for pure climatology). The residuals for this case are nearly indistinguishable from the residuals of the GAM without AOD observations discussed above. Adding in additional satellite variables adds little to the predictive ability of the model. This is consistent with the low initial correlation of the GOES AOD and hourly $PM_{2.5}$ and suggests that the AOD observations provide little ability to predict surface $PM_{2.5}$ during potentially smoky periods. Looking at the functional fit of GOES AOD (Figure 7) shows that GOES AOD is linearly proportional with $PM_{2.5}$ up to AOD values of 0.2, at which point the functional relationship reverses, suggesting that AOD and surface $PM_{2.5}$ are less likely to be linked at high AOD values.

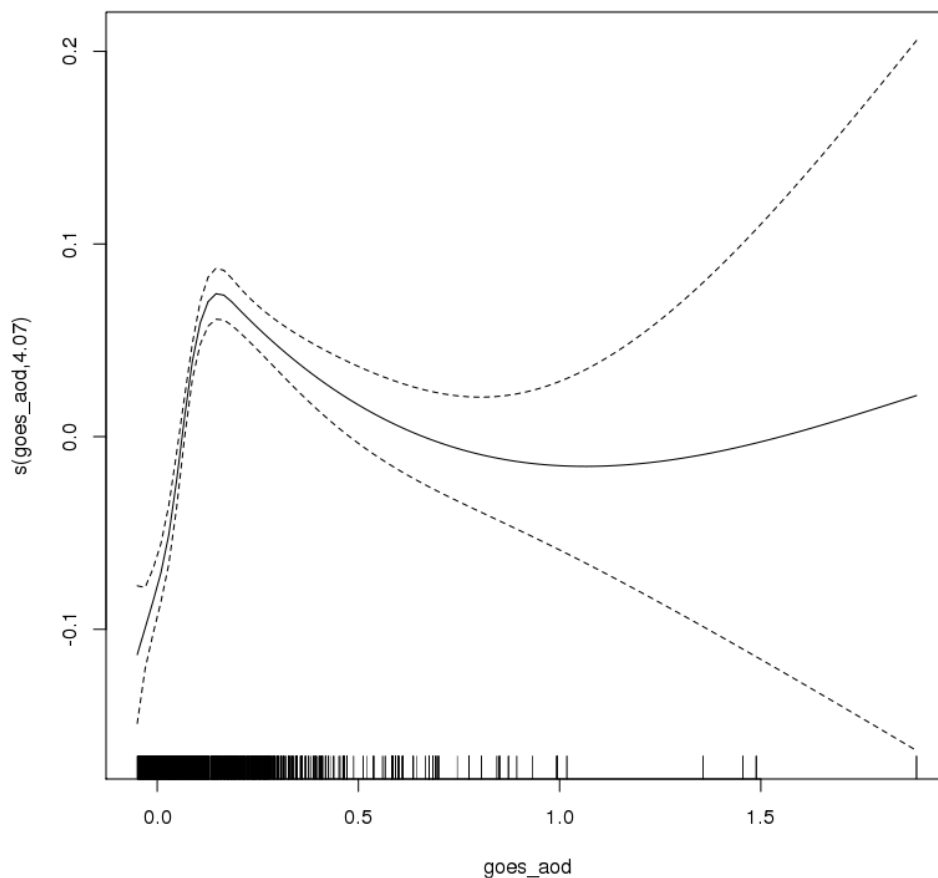


Figure 7. Smooth functional fit of GOES AOD to $PM_{2.5}$ in GAM. Dashed lines are the 1-sigma uncertainty of the fits.

Given these discouraging results, we have not further pursued the ability of the satellite observations discussed in Section 2 to predict surface level $PM_{2.5}$. Any further work done after this draft final report will be included in the final project report.

6 Audits of Data Quality and Reconciliation with User Requirements

No project-specific quality requirements exist for the information that will be used in this project. All data used in this project was filtered using the quality flags as directed by the respective data user's guides. The processing and analysis scripts used in this project were inspected by a team member not involved in their creation for accuracy. All automated calculations and at least 10% of manual calculations were inspected for correctness, meeting the requirement of Level III QAPPs that 10% of the data must be inspected. No significant errors were found.

In addition, the QAPP listed the following quality assessment questions:

- *Do the relationships described in the developed models make physical sense given our conceptual models of smoke transport, AOD, and surface PM_{2.5}?*

As the analysis in Task 3 showed little correlation between GOES AOD and surface PM_{2.5}, no significant details of the relationship could be reached,

- *Are these relationships consistent with the scientific literature?*

As noted above, little relationship was found between the different satellite parameters and surface PM_{2.5} concentrations.

- *Under what conditions are the models expected to be valid? What conditions give exceptionally large residuals?*

The current Task 3 models only explain 34% of the variability in surface PM_{2.5} and have significant residuals under all conditions.

- *What are the bias and error characteristics of the models?*

While the models are unbiased (mean residuals of 0), they have significant scatter in the residuals (standard deviation of $\sim 5 \mu\text{g}/\text{m}^3$) that makes them less useful for PM_{2.5} prediction.

7 Conclusions

Here we summarize the conclusions of our project, with reference to the corresponding report section.

- A sampling of three NRT smoke products in the Texas/Gulf of Mexico region indicates little spatial agreement in presence of smoke and/or horizontal extent (Section 2).
- Using NRT product overlap on a common spatial grid (GOES 2km) suggests greater predictive power for smoke presence. Combining the overlapping products into a simple smoke confidence index is potentially valuable (Section 2).
- Incorporating additional remotely-sensed smoke-relevant variables such as NH_3 , CO, and Brown Carbon into a smoke presence analysis adds further value to assessing presence and/or horizontal extent of smoke (Section 2).
- Smoke flags in the Texas/Gulf of Mexico region are skewed toward more data from GOES and HMS.
- There is a significant positive correlation between higher AOD and higher SCI values lending increased confidence in the power of combining smoke product information (Section 2, 3)
- For higher confidence smoke pixels ($\text{SCI} \geq 2$), a MAIAC-derived relationship between AOD and plume height provides a baseline estimate for smoke plume height (Section 3)
- All smoke relevant indicators (including the SCI) are positively correlated with increased smoke activity during the peak Texas/Gulf of Mexico biomass burning months of April and May (Section 2, 3).
- GOES AOD and other satellite smoke predictors had little correlation ($r < 0.2$) with hourly surface $\text{PM}_{2.5}$ in Texas urban areas, and so statistical models gave generally poor predictions (adj. $R^2 < 0.35$, standard deviation of residuals of $\sim 5 \mu\text{g}/\text{m}^3$) (Section 5).

8 Recommendations for Further Study

We recommend the following items for further study:

- How smoke-threshold UVAI is selected should be revisited. Studies suggest that agricultural fires have a weaker signal. An examination of smoke-impacted UVAI by CONUS vegetation type burned will be valuable.
- How the SCI is calculated should be revisited. A simple smoke product overlap system can be replaced with a more sophisticated metric that includes the NH₃, CO, BrC, and AOD inputs. Currently, due to a lower UVAI sample size, an SCI of “3” is rare and not particularly informative.
- For FMS calculations, a daily “radius” approach can be developed and applied in addition to a simple hourly pixel-by-pixel matching approach as the latter tends to underestimate product similarities. For instance, if two products have smoke identified in a certain radius but the exact pixel locations do not match, the FMS would misleadingly be 0.
- AOD measurements are frequently missing. In the future, the AOD selection criteria can be revisited such that we accept both “medium” and “good” quality GOES AOD. In addition, hourly averages can be calculated when 50% (6 files) of AOD data quality is met per pixel per hour rather than 75% (9 files).
- The GOES and HMS smoke data from this study, along with processing methodology, was leveraged in a recent TCEQ-funded study exploring machine learning techniques for enhanced NRT smoke identification (Brown Steiner *et al.*, 2021). Early results from that TCEQ study were promising, and future versions of the machine learning approach could benefit from incorporating additional smoke-related metrics and tools identified in this AQRP study.

9 References

- Ahmadov, R., Grell, G., James, E., Freitas, S., Pereira, G., Csiszar, I., Tsidulko, M., Pierce, B., McKeen, S., Peckham, S., Alexander, C., Saide, P., and Stan, B. (2017), A high-resolution coupled meteorology-smoke modeling system HRRR-Smoke to simulate air quality over the CONUS domain in real time. In *EGU General Assembly Conference Abstracts* (Vol. 19, p. 10841).
- Akagi, S. K., Yokelson, R. J., Wiedinmyer, C., Alvarado, M. J., Reid, J. S., Karl, T., Crounse, J. D., and Wennberg, P. O. (2011), Emission factors for open and domestic biomass burning for use in atmospheric models, *Atmos. Chem. Phys.*, **11**, 4039–4072, doi:10.5194/acp-11-4039-2011.
- Alvarado, M.J. and Dayalu, A (2020), *Tracking Brown Carbon with Satellite Imagery*, Data Documentation and Users' Guide to Accompany Final Report to Texas Commission on Environmental Quality (TCEQ) for Work Order No. 582-20-12438-006 under TCEQ Contract No. 582-19-90498, Aug 15.
- Alvarado, M.J. and Dayalu, A (2021), *Tracking Brown Carbon with Satellite Imagery*, Final Report to Texas Commission on Environmental Quality (TCEQ) for Work Order No. 582-20-12438-006 under TCEQ Contract No. 582-19-90498, May 24.
- Alvarado, M. J., Cady-Pereira, K. E., Xiao, Y., Millet, D. B., and Payne, V. H. (2011), Emission ratios for ammonia and formic acid and observations of peroxy acetyl nitrate (PAN) and ethylene in biomass burning smoke as seen by the tropospheric emission spectrometer (TES), *Atmosphere*, **2**, 633–654, doi:10.3390/atmos2040633.
- Brey, S. J., Ruminski, M., Atwood, S. A., and Fischer, E. V. (2018), Connecting smoke plumes to sources using Hazard Mapping System (HMS) smoke and fire location data over North America, *Atmos. Chem. Phys.*, **18**, 1745–1761, <https://doi.org/10.5194/acp-18-1745-2018>.
- Brown-Steiner, B., Lonsdale, C., Hegarty, J., and Alvarado, M. (2018), *Assessment of the Exceptional Event Rule's 'Q/D' Guidance*, Final Report to Texas Commission on Environmental Quality (TCEQ) for Work Order No. 582-18-81899-09 under TCEQ Contract No. 582-15-50414, June 29.
- Brown-Steiner, B., Dayalu, A., and Alvarado, M. (2019), *Uncertainty analysis and improvement of STILT-ASP for determining O3 formation from biomass burning*, Final Report to Texas Commission on Environmental Quality (TCEQ) for Work Order No. 582-19-92805-03 under TCEQ Contract No. 582-19-90498, June 30.
- Brown-Steiner, B., Dayalu, A., Ashok, A., and Alvarado, M. (2021), *Wildfire Smoke Tracking Algorithm*, Final User's Guide and Brief Technical Memo to Texas Commission on Environmental Quality (TCEQ) for Work Order No. 582-21-22400-007 under TCEQ Contract No. 582-19-90498, June 30.
- Cheeseman, M., Ford, B., Volckens, J., Lyapustin, A., & Pierce, J. R. (2020). The relationship between MAIAC smoke plume heights and surface PM. *Geophysical Research Letters*, 47, e2020GL088949. <https://doi.org/10.1029/2020GL088949>
- GOES-R Users' Guide (2019). GOES-R Series Product Definition and Users' Guide. 416-R-PUG-L2 Plus-0349 Vol 5, Rev. 2.2. <https://www.goes-r.gov/products/docs/PUG-L2+-vol5.pdf>.

- Goldberg, D. L., Gupta, P., Wang, K., Jena, C., Zhang, Q., Martin, R. V., van Donkelaar, A., Huo, H., Che, H., Lin, Y., Lu, Z., and Streets, D. G. (2019), Using gap-filled MAIAC AOD and WRF-Chem to estimate daily & He, K. (2015). Estimating long-term PM_{2.5} concentrations at 1 km resolution in the Eastern United States, *Atmospheric Environment*, **199**, 443–452.
- Hu, X., Yu, C., Tian, D., Ruminski, M., Robertson, K., Waller, L. A., in China using satellite-and Liu, Y. (2016), Comparison of the Hazard Mapping System (HMS) fire product to ground-based fire records in Georgia, USA, *J. Geophys. Res.-Atmos.*, **121**, 2015JD024448, <https://doi.org/10.1002/2015JD024448>.
- Lee, H. J., Liu, Y., Coull, B. A., Schwartz, J., and Koutrakis, P. (2011), A novel calibration approach of MODIS AOD data to predict PM_{2.5} concentrations, *Atmospheric Chemistry & Physics*, **11**(15).
- Lonsdale, C. R., Alvarado, M. J., Yokelson, R. J., Travis, K. R., and Fischer, E. V. (2014), A sub- grid scale parameterization of biomass burning plume chemistry for global and regional air quality models, presented at the 2014 Community Modeling and Analysis System (CMAS) Conference, Chapel Hill, NC, 27-29 Oct.
- Lonsdale, C. R., Hegarty, J. D., Cady-Pereira, K., Alvarado, M. J., Henze, D. K., Turner, M. D., Capps, S. L., Nowak, J. B., Neuman, J. A., Middlebrook, A. M., Bahreini, R., Murphy, J. G., Markovic, M., VandenBoer, T. C., Russell, L. M., and Scarino, A. J. (2017a), Modeling the diurnal variability of agricultural ammonia in Bakersfield, California during CalNex, *Atmos. Chem. Phys.*, **17**, 2721–2739, doi:10.5194/acp-17-2721-2017.
- Lonsdale, C. R., Brodowski, C. M., and Alvarado, M. J. (2017b), *Improving the Modeling of Wildfire Impacts on Ozone and Particulate Matter for Texas Air Quality Planning*, Final Report to Texas Air Quality Research Program (AQR) Project 16–024, August 31.
- Lv, B., Hu, Y., Chang, H. H., Russell, A. G., and Bai, Y. (2016), Improving the accuracy of daily PM_{2.5} distributions derived from the fusion of ground-level measurements with aerosol optical depth and a chemical transport model. *Remote Sensing of Environment*, **166**, 262–270. observations, a case study in North China, *Environmental Science & Technology*, **50**(9), 4752–4759.
- Lyapustin, A., Wang, Y., Korkin, S., Kahn, R., and Winker, D. (2019), MAIAC Thermal Technique for Smoke Injection Height from MODIS, *IEEE Geoscience and Remote Sensing Letters*, 2019 Sep 12.
- Lyapustin, A., Martonchik, J., Wang, Y., Laszlo, I., and Korkin, S. (2011), Multiangle implementation of atmospheric correction (MAIAC): 1. Radiative transfer basis and look-up tables, *Journal of Geophysical Research: Atmospheres*, **116**(D3), D21201.
- McDonald-Buller, E., Y. Kimura, C. Wiedinmyer, C. Emery, Z. Liu, and G. Yarwood (2015), *Targeted Improvements in the Fire Inventory from NCAR (FINN) Model for Texas Air Quality Planning*, Final Report to Texas Air Quality Research Program (AQR) for Project 14-011, December 2015.
- Nelson, D., Garay, M., Kahn, R., and Dunst, B. (2013), Stereoscopic height and wind retrievals for aerosol plumes with the MISR INteractive eXplorer (MINX). *Remote Sensing*, **5**(9), 4593–4628.

- NOAA/NESDIS/STAR (2018), Algorithm theoretical basis document: ABI aerosol detection product. Available at https://www.star.nesdis.noaa.gov/goesr/documents/ATBDs/Baseline/ATBD_GOES-R_Aerosol_Detection_v3.0_Jan2019.pdf (last access: 11 January 2020).
- Rolph, G. D., Draxler, R. R., Stein, A. F., Taylor, A., Ruminski, M. G., Kondragunta, S., Zeng, J., Huang, H.-C., Manikin, G., McQueen, J. T., and Davidson, P. M. (2009), Description and verification of the NOAA smoke forecasting system: The 2007 fire season, *Weather Forecast.*, **24**, 361–378, <https://doi.org/10.1175/2008WAF2222165.1>.
- Ruminski, M., Kondragunta, S., Draxler, R., and Zeng, J. (2006), Recent changes to the Hazard Mapping System, 15th Int. Emiss. Inventory Conf, (Reinventing Inventories), available at: https://www.researchgate.net/publication/228625934_Recent_changes_to_the_Hazard_Mapping_System (last access: 11 January 2020).
- Schroeder, W., Ruminski, M., Csiszar, I., Giglio, L., Giglio, E., Schmidt, C., and Morisette, J. (2008), Validation analyses of an operational fire monitoring product: The Hazard Mapping System, *Int. J. Remote Sens.*, **29**, 6059–6066.
- Shephard, M. W., A., Martin, R. V., Brauer, M., Kahn, R., Levy, and Cady-Pereira, K. E. (2015), Cross-track Infrared Sounder (CrIS) satellite observations of tropospheric ammonia, *Atmos. Meas. Tech.*, **8**, 132–1336, doi:10.5194/amt-8-1323-2015.
- Soja, A. J., Choi, H. D., Fairlie, T. D., Pouliot, G., Baker, K. R., Winker, D. M., Trepte, C. R., and Szykman, J. (2017), CALIOP-based Biomass Burning Smoke Plume Injection Height. In *AGU Fall Meeting Abstracts*.
- Sorek-Hamer, M., Strawa, A. W., Chatfield, R. L., B., Esswein, R., Cohen, A., & Broday, D. M. (2013). Improved retrieval of PM_{2.5} from satellite data products using non-linear methods. *Environmental Pollution*, **182**, 417–423.
- Sorek-Hamer, M., Kloog, I., Koutrakis, P., Strawa, A., Chatfield, R., Cohen, A., Ridgway, W., ground-level PM_{2.5} & Broday, D. M. (2015). Assessment of PM_{2.5} concentrations at 4 km resolution over bright surfaces using Beijing-Tianjin-Hebei by fusing MODIS satellite AOD and ground observations. *Remote Sensing, Science of the Total Environment*, **163**, 180–185. **580**, 235–244.
- Stein, A. F., Rolph, G. D., Draxler, R. R., Stunder, B., and Ruminski, M. (2009), Verification of the NOAA smoke forecasting system: model sensitivity to the injection height, *Weather and Forecasting*, **24**(2), 379–394.
- Strawa, A. W., Chatfield, R. B., Legg, M., Scarnato, B., & Esswein, R. (2013). Improving retrievals of regional fine particulate matter concentrations from Moderate Resolution Imaging Spectroradiometer (MODIS) and Ozone Monitoring Instrument (OMI) multisatellite observations. *Journal of the Air & Waste Management Association*, **63**(12), 1434–1446.
- Vadrevu K., Lasko, K., Giglio, L., and Justice, C. (2015). Vegetation fires, absorbing aerosols and smoke plume characteristics in diverse biomass burning regions of Asia. *Environ. Res. Lett.* **10** 105003. <http://iopscience.iop.org/1748-9326/10/10/105003>

- VanVerduzco, C., & Villeneuve, P. J. (2010). Global estimates of ambient fine particulate matter concentrations from satellite-based aerosol optical depth: development and application. *Environmental Health Perspectives*, 118(6), 847–855.
- van Donkelaar, A., Martin, R. V., & Park, R. J. (2006). Estimating ground-level PM_{2.5} using aerosol optical depth determined from satellite remote sensing.
- van Donkelaar, Martin, R. V., Levy, R. C., da Silva, A. M., Krzyzanowski, M., Chubarova, N. E., Semutnikova, & Cohen, A. J. (2011). Satellite-based estimates of ground-level fine particulate matter during extreme events: A case study of the Moscow fires in 2010. *Atmospheric Environment*, 45(34), 6225–6232.
- van Donkelaar, A., Martin, R. V., Spurr, R. J., Drury, E., Remer, L. and Levy, R. C., & Wang, J. (2013). Optimal estimation for global ground-level fine particulate matter concentrations. *Journal of Geophysical Research: Atmospheres*, 118(11), 5621–5636.
- van Donkelaar, A., Martin, R. V., Brauer, M., & Boys, B. L. (2015a). Use of satellite observations for long-term exposure assessment of global concentrations of fine particulate matter. *Environmental Health Perspectives*, 123(2), 135–143.
- van Donkelaar, A., Martin, R. V., Spurr, R. J., & Burnett, R. T. (2015b). 2015), High-resolution satellite-derived PM_{2.5} from optimal estimation and geographically weighted regression over North America., *Environmental Science & Technology*, 49(17), 10482–10491.
- Wood, S. N. (2006), *Generalized Additive Models: An Introduction with R*, part of the “Texts in Statistical Science” series, Chapman & Hall/CRC, New York.

- Wang, X., Heald, C. L., Sedlacek, A. J., de Sá, S. S., Martin, S. T., Alexander, M. L., Watson, T. B., Aiken, A. C., Springston, S. R., and Artaxo, P. (2016), Deriving brown carbon from multiwavelength absorption measurements: method and application to AERONET and Aethalometer observations, *Atmos. Chem. Phys.*, **16**, 12733–12752, <https://doi.org/10.5194/acp-16-12733-2016>.
- Wang, Y., and Talbot, R. (2017), *High Background Ozone Events in the Houston-Galveston- Brazoria Area: Causes, Effects, and Case Studies of Central American Fires*. Final Report to Texas Air Quality Research Program (AQRP) Project 16 – 008, October.
- Zeng, J., and S. Kondragunta (2010), Tracking Smoke Plumes Using GOES Imagery. In *17th Conference on Satellite Meteorology and Oceanography*. Available at https://ams.confex.com/ams/17Air17Sat9Coas/techprogram/paper_174773.htm (last access: 11 January 2020).
- Zhang, K., de Leeuw, G., Yang, Z., Chen, X., Su, X., and Jiao, J. (2019), Estimating spatio- temporal variations of PM_{2.5} concentrations using VIIRS-derived AOD in the Guanzhong Basin, China, *Remote Sens.*, **11**, 2679.

Appendix A: Flowchart of processing code and output

